Numerical investigation of gaseous detonation instability observed in the elastoplastically deforming metal confinements

Min-cheol Gwak[1] and Jack J. Yoh[1]
[1]School of Mechanical and Aerospace Engineering, Seoul National University
1 Gwanakro, Gwanakgu, Seoul, Korea 151-744

1 Introduction

Detonation wave is a reactive shock wave supported by the rapid chemical reaction that results in a sudden increase of pressure and temperature, leading to an extreme thermodynamic state within a very short time. When accompanied by structural deformation or a failure, such transition to a detonation in structures can raise a major safety concern. For instance, internal detonation of a fuel transporting pipe line may trigger pipe rupture and a catastrophic disaster by an explosion [1, 2]. An industrial application in tube forming via the gaseous detonation process is an alternative and practical use of such complex reactive phenomena [3]. In other words, if properly understood and controlled, the interaction between the gaseous detonation and the confinement structures may provide a remedy for future prevention of accidental explosion or enhancement of the efficiency associated with explosive forming.

In this paper, we investigate the effect of wall expansion on the detonation transition in different metal tubes as similarly used in rate stick tests of [4]. An effect of strong coupling between the exploding gas (ethylene-air mixture) and the elasto-plastic confinement is observed on the basis of a numerical simulation. For handling of complex fluid-structure issues involving detonations, hydrocode in the Arbitrary Largrangian Eulerian framework has been used by others [5,6], where as in this work, we adapt an innovative Eulerian approach combined with the hybrid particle level sets and the ghost fluid interface technique [4] to simulate the dynamic response of plastically deforming walls exposed to a detonating internal gas flow. We consider three types of metals (tungsten, copper, and aluminum) along with five different tube thicknesses (0.8, 1, 1.2, 1.4, 1.6 mm). The simulated responses are then compared with analytical behaviors [7] for confirming predictions achieved by the present approach.

2 Numerical strategy

2. 1 Governing equations

To simulate behaviors of deformable tube under detonation loading, we used the conservative laws of mass, momentum, energy and chemical species in axisymmetric cylindrical coordinate shown in eqns. (1)-(5).

Correspondence to: jjyoh@snu.ac.kr (Jack J. Yoh)

$$\frac{\partial \rho}{\partial t}+\frac{\partial}{\partial r}\left(\rho u_r\right)+\frac{\partial}{\partial z}\left(\rho u_z\right)+\frac{\rho u_r}{r}=0 \tag{1}$$

$$\frac{\partial}{\partial t}\left(\rho u_r\right)+\frac{\partial}{\partial r}\left(\rho u_r{}^2+P\right)+\frac{\partial}{\partial z}\left(\rho uv\right)-\frac{\tau_{rr}-\tau_{\theta\theta}-\rho u_r^2}{r}-\frac{\partial \tau_{rr}}{\partial r}-\frac{\partial \tau_{rz}}{\partial z}=0 \tag{2}$$

$$\frac{\partial}{\partial t}\left(\rho u_z\right)+\frac{\partial}{\partial r}\left(\rho u_r u_z\right)+\frac{\partial}{\partial z}\left(\rho u_z{}^2+P\right)-\frac{s_{zr}-\rho u_r u_z}{r}-\frac{\partial \tau_{rz}}{\partial r}-\frac{\partial \tau_{zz}}{\partial z}=0 \tag{3}$$

$$\begin{aligned}\frac{\partial}{\partial t}\left(\rho e\right)+\frac{\partial}{\partial r}\left[u_r\left(\rho e+P\right)\right]+\frac{\partial}{\partial z}\left[u_z\left(\rho e+P\right)\right]-\frac{u_r\tau_{rr}+u_z\tau_{rz}-q_r-u_r(\rho e+p)}{r}\\ -\frac{\partial\left(u_r\tau_{zr}+u_z\tau_{zz}-\varphi q_z\right)}{\partial z}-\varphi\rho Q_i\dot{w}_i-\frac{\partial\left(u_r\tau_{rr}+u_z\tau_{rz}-\varphi q_r\right)}{\partial r}=0\end{aligned} \tag{4}$$

$$\varphi\left\{\frac{\partial}{\partial t}\left(\rho Y_i\right)+\frac{\partial}{\partial r}\left(\rho Y_i u_r\right)+\frac{\partial}{\partial z}\left(\rho Y_i u_z\right)+\frac{d_r}{r}+\frac{\partial d_r}{\partial r}+\frac{\partial d_z}{\partial z}-\rho\dot{w}_i\right\}=0 \tag{5}$$

where φ = 0 or 1 for a ductile metal (deformable tube) or a reactive gas, respectively. In these equations ρ, u_r, u_z, P, e, and Y_i are density, r-axis velocity, z-axis velocity, pressure, total energy density, and mass fraction of reactant, respectively. Also $\vec{q}=k\nabla T$ is the thermal conduction, $\dot{w}_i \equiv \partial Y_i/\partial t\big|_{Chem}=A\rho Y\exp\left(-E_a/(RT)\right)$ is the reaction rate described by the first-order Arrhenius kinetics, and $\vec{d}=\rho D\nabla Y_i$ is the mass diffusion. Here, k is the thermal conduction coefficient, A is the pre-exponential factor, E_a is the activation energy, and D is the mass diffusion coefficient. We use the coefficients of kinematic viscosity, diffusion, and heat conduction that depend on the temperature such that $\mu=\nu_0 T^n$, $D=D_0T^n/\rho$, $k/\left(\rho c_P\right)=k_0T^n/\rho$. The ν_0, D_0, and k_0 are constants, $c_P=\gamma R/M\left(\gamma-1\right)$ is the specific heat at constant pressure, and n=0.7. Also, non-dimensional Lewis, Prandtl, and Schmidt numbers are assumed to be unity [3], as these assumptions do not affect the physics of detonation propagation in the relevant medium. Within the combustible gas mixture, deviatoric (viscous) stresses, τ_{rr}, $\tau_{rz}=\tau_{zr}$, and τ_{zz} are calculated based on the constitutive relation for a Newtonian fluid. As for the deformable tube, deviatoric stresse fields are calculated together with the evolution equations based on a Hooke's law and the flow theory of plasticity for high strain rate deformation [6].

To solve the entire governing equations, convection is handled by the Essentially Non-Oscillatory (ENO) scheme for spatial discretization, and a third-order Runge-Kutta (RK) integration is used for time stepping of the resulting system of ordinary differential equations [8]. In addition, the second-order fluxes of viscocity, heat conduction, and mass diffusion are evaluated by the second-order differences. The spatial resolution of 0.2 mm allows correct pressure and density to be obtained in combustible gas and deformable wall regions [9].

2.2 Constitutive relations

The pressure of combustible gas mixture is calculated by the ideal gas equation of state (EOS), $P=\rho RT/M$ [10]. Here, R and M are universal gas constant and molecular weight, respectively. For description of the deformable tube, we use Mie-Gruneisen EOS and rate-dependent Johnson-Cook strength model in which the yield stress depends on shear rate and temperature shown in eqns. (6) and (7) below:

$$\sigma_Y=\left(\sigma_{Y,0}+A\left(\bar{\varepsilon}^P\right)^n\right)\left(1+B\ln\left(\frac{\dot{\bar{\varepsilon}}^P}{\dot{\varepsilon}_0}\right)\right)\left(1-\left(\frac{T-T_0}{T_m-T_0}\right)^m\right) \tag{6}$$

$$p(\rho,e)=\rho_0\Gamma_0 e+\begin{cases}\dfrac{\rho_0 c_0^2\varphi}{(1-s\varphi)^2}\left[1-\dfrac{\Gamma_0}{2}\varphi\right] & \text{if } \rho\geq\rho_0\\ c_0^2\left(\rho-\rho_0\right) & \text{otherwise}\end{cases},\ \varphi=1-\frac{\rho_0}{\rho} \tag{7}$$

where A, B, n, c_0, and s are material constants, and T_m, T_0 are melting and ambient temperatures.

3 Numerical setup

In this study, we consider ethylene-air mixture as the fuel-air mixture and tungsten, copper, aluminum as three different metals subject to a detonation loading. Table 1 and 2 show the initial conditions and the parameters of gaseous mixture and the metal tubes.

Table 1: Initial conditions and parameters of ethylene-air mixture

Initial temperature (T_0)	293 K
Initial pressure (P_0)	$1.33\text{x}10^4$ Pa
Initial density (ρ_0)	$1.58\text{x}10^{-1}$ kg/m^3
Specific heat ratio (γ)	1.15
Molecular weight (M)	$29\text{x}10^{-3}$ kg/mol
Pre-exponential factor (A)	$3.2\text{x}10^8$ m^3/(kg s)
Activation energy (E_a)	$35.3514RT_0$
Chemical energy release (q)	$48.824RT_0/M$
CJ detonation pressure	$1.2\text{x}10^6$ Pa
CJ detonation velocity	1870 m/s

Table 2: Parameters of ductile metal tubes [11]

	Tungsten	Copper	Aluminum
Initial density (ρ_0)	17600 kg/m^3	8930 kg/m^3	2700 kg/m^3
Young's modulus (E)	200 GPa	117 GPa	70 GPa
Possions ratio (γ)	0.29	0.35	0.35
Heat capacity (c)	477 W/(m K)	383.5 W/(m K)	1000 W/(m K)
Thermal conductivity (k)	38 J/(kg K)	401J/(kg K)	170 J/(kg K)
Melting temperature (T_m)	1777 K	1358 K	855 K
Gruneisen coefficient (Γ)	1.43	2.0	2.0
Normal sound speed (c_0)	4030 m/s	3940 m/s	5328 m/s
s	1.237	1.49	1.338
Initial yield strength ($\sigma_{Y,0}$)	1.51 GPa	0.4 GPa	0.255 GPa
A	0.177 GPa	0.1 GPa	0.3277 GPa
n	0.12	1.0	1.008
B	0.016	0.025	0.00747
m	1.00	1.09	1.31

The computational domain is shown in Fig. 1, where a section of the shock tube (250 mm by 25 mm) is considered with five different tube thicknesses (0.8, 1, 1.2, 1.4, 1.6 mm). The boundary conditions include zero gradient inflow conditions on both ends while a symmetry condition is imposed on the upper side. As for initiating detonation, a CJ condition is used at the bottom boundary. In particular, the deforming material interfaces that separate internal combustion gas from metal, and metal from external void are tracked via the hybrid particle level-set method in the framework of ghost fluid method [6].

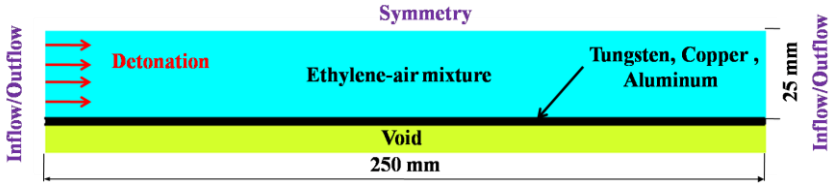

Figure 1. Initial numerical setup

4 Results

4.1 Deformable metal tube under detonation loading

To confirm deformation of tube being an elasto-plastic material subject to a detonation loading, we consider a thin metal tube filled with the ethylene-air mixture. Figure 2 shows images of an outbreak of wall expansion wave from a wall position where the effective plastic stress ($\overline{\sigma} = \sqrt{3\left(\tau_{rr}^2 + \tau_{zz}^2 + \tau_{rr}\tau_{zz} + \tau_{rz}^2\right)}$) exceeds yield stress.

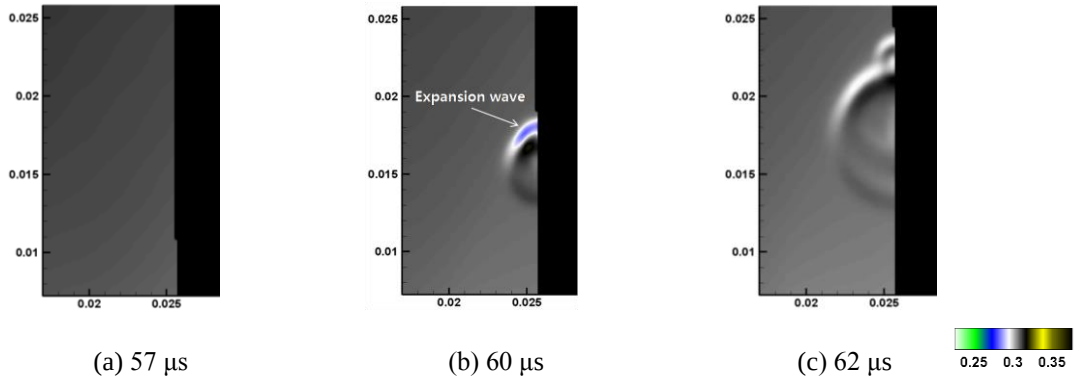

(a) 57 μs (b) 60 μs (c) 62 μs

Figure 2. Density fields (unit: kg/m^3) of ethylene-air mixture confined in 1 mm thin copper tube. First outbreak of wall expansion is marked at the location where effective plastic stress exceeds the copper yield stress.

The acoustic pressure wave from the wall expansion is approximately 0.85 times the ambient detonation pressure which then introduces strong non-uniformity to density field. As these wall expansion generated Mach waves continue to appear over time, they start to merge and form compression waves that give rise to a rich cellular structure shown in the Fig. 3. Only source of disturbance responsible for such instability is the wall expansion, and thus no a-priori numerical 'jitter' or sinusoidal flow disturbance was used to initialize the flow simulation. Figure 3 also describes regions of decreased density due to a volume increase from expansion of burnt gas while the propagating detonation wave structure resembles a multi-cellular structure typically seen from propagating detonation of hydrocarbon fuel-air mixture in channel. We have made use of effective plastic strain rate (EPSR) as a measure of plastic state of deformation as such the EPSR being zero means zero deformation. Figure 4 depicts the calculated EPSR at 120 μs, and it is gradually increasing toward the lower side of the expanding tube.

4.2 Critical tube thickness

We consider the relationship between the tube thickness and deformation under the detonation loading. A theoretical deformable thickness and a shakedown pressure [7] can be obtained. Figure 5 shows tube expansion ratios in the case of copper tube for five different thicknesses (0.8, 1, 1.2, 1.4, 1.6 mm). Here the start time of wall expansion is delayed with the slower rate of expansion as the tube thickness is increased. When 1.6 mm or bigger tube thickness is considered, there is no expansion with only a minor wall fluctuation (in a separate window) noted, since the loading pressure did not exceed

the yield strength of a copper. This suggests the existence of a critical thickness between 1.4 and 1.6 mm that defines a threshold or shakedown pressure as given by a simple analytical expression,

$$p_S = 2\sigma_Y \frac{2r_i t + t^2}{\beta\sqrt{3(r_i + t)^4 + r_i^4}} \tag{8}$$

The shakedown pressure is determined by r_i, inner radius, t, thickness, β, dynamic amplification factor, and σ_Y, yield stress of tube. By using the detonation pressure of ethylene-air as a shakedown pressure, the critical thickness of copper tube can be calculated as 1.42 mm, which is in good agreement with the present numerical simulation.

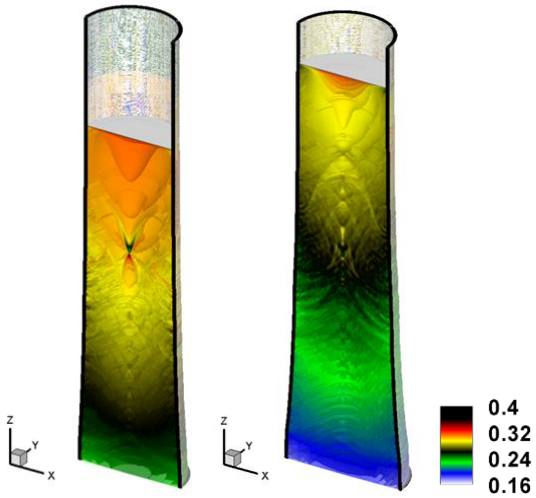

Figure 3. Density fields (unit: kg/m^3) of ethylene-air mixture in 1 mm thin copper tube

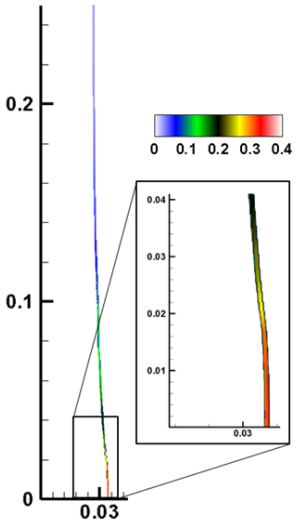

Figure 4. Effective plastic strain rate (EPSR) in 1 mm thickness copper tube at 120 μs

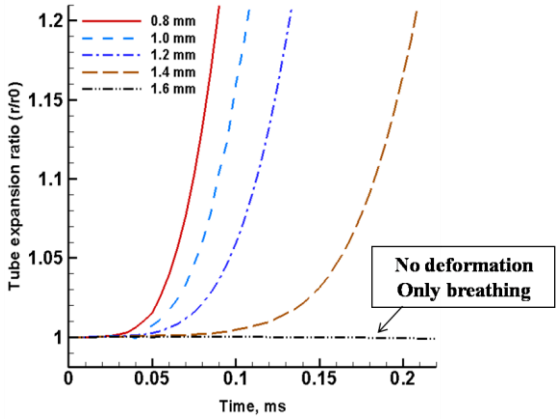

Figure 5. Tube expansion ratios of copper tubes with five different thicknesses (0.8, 1, 1.2, 1.4, 1.6 mm)

4. 3 Difference in metal tubes

Different metals (tungsten, copper, and aluminum) are considered for understanding of material dependent issues associated with detonating pipe simulations. In the case of aluminum tube, dynamic elasto-plastic response under detonation is seen most sensitive among other two metals due to its low density and yield strength. Tungsten on the other hand showed the least sensitivity (Fig. 6). Figure 7 shows expansion ratios of all three metals under the detonation loading plotted in time. The expansion

ratio of tungsten is marked by the slowest expansion due to its high initial yield strength; however, the rate of expansion (or the slope) is more rapid than copper tube suggesting its lower thermal conductivity and lower sensitivity to yield at a higher temperature. All three metals behave consistent with the engineering notion, and the calculated results seem plausible. For quantitative analysis, comparison to experimental data is necessary.

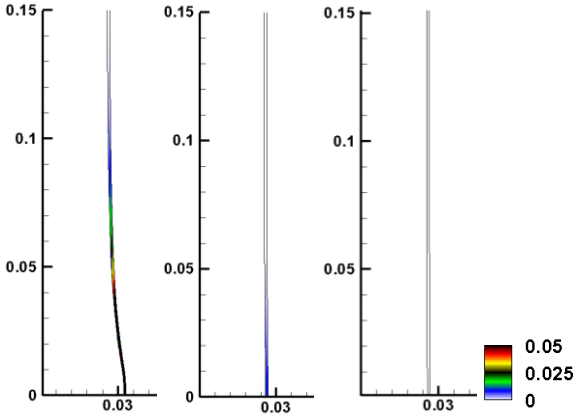

(a) Aluminum (b) Copper (c) Tungsten

Figure 6. Effective plastic strain of 1 mm tube calculated at 60 μs under static detonation loading condition (P/P_0=62.45)

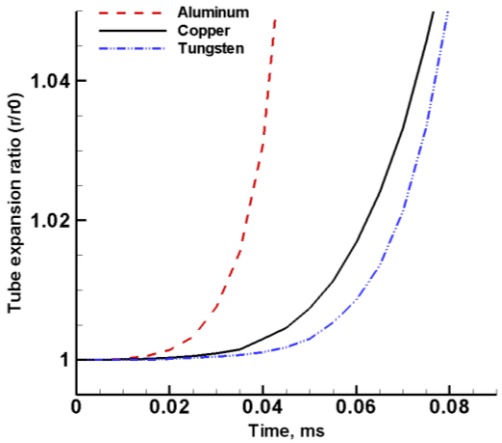

Figure 7. Histories of tube expansion ratio under static detonation loading condition (P/P_0=62.45)

5 Conclusions

A careful evaluation of the wall boundary conditions and deformation response of ductile tube is performed in the context of multi-material high-strain rate phenomena involving combustion gas and its interaction with the confinements. We confirm that calculated response of various metal tubes under detonation loading using a high order multi-material method is consistent with the pipe failure theory. The present method that solves the continuum balance laws of detonation and elasto-plastically deforming boundary conditions is capable of predicting the dynamic response of metal tube subject to an internal detonation or a DDT loading.

Acknowledgment

The authors are thankful for financial support from the Agency for Defense Development through the Institute of Advanced Aerospace Technology at Seoul National University.

References

[1] Naitoh M et al. (2003). Analysis on pipe rupture of steam condensation line at hamaoka-1, (II). J. Nuclear. Sci. Tech. 40(12): 1041

[2] Vaidogas ER, Juocevicius V. (2008). Sustainable development and major industrial accidents: The beneficial role of risk-oriented structural engineering. Tech. Economic Devel. Economy 14(4): 612

[3] Kleiner M et al. (2007). Tube expansion by gas detonation. Prod. Eng. Res. Devel. 1: 9

[4] Kim K, Yoh JJ. (2013). A particle level-set based Eulerian method for multi-material detonation simulation of high explosive and metal confinements. Proc. Combust. Inst. 34: 2025

[5] Benson DJ. (1992). Computational methods in Lagrangian and Eulerian hydrocodes. Comput. Methods Appl. Mech. Eng. 99: 235

[6] Liu WK et al. (1986). An arbitrary lagrangian-eulerian finite element method for path-dependent materials. Methods Appl. Mech. Eng. 58: 227

[7] Zhao W et al. (2003). On thick-walled cylinder under internal pressure. J. Pre. Vessel Tech. 125: 267

[8] Liu X, Osher S. (1998). Convex ENO high order multi dimensional schemes without field by field decomposition or staggered grid. J. Comput. Phys. 147: 1-27

[9] Shepherd JE et al. (2009). Gaseous detonation in piping systems partially filled with liquid. Proc. ASME PVP2009. PVP2009-77734

[10] Oran ES, Gamezo VN. (2007). Origins of the deflagration-to-detonation transition in gas-phase combustion. Combust. Flame 148: 4

[11] Tran LB, Udaykumar HS. (2004). A particle-level set-based sharp interface cartesian grid method for impact, penetration, and void collapse. J. Comput. Phys. 193: 469-510